

Stem Cell Reports, Volume 10

Supplemental Information

**Contractile Work Contributes to Maturation of Energy Metabolism in
hiPSC-Derived Cardiomyocytes**

Bärbel M. Ulmer, Andrea Stoehr, Mirja L. Schulze, Sajni Patel, Marjan Gucek, Ingra Mannhardt, Sandra Funcke, Elizabeth Murphy, Thomas Eschenhagen, and Arne Hansen

Supplemental Information

Supplemental Figures 1-7

A

	Control cell line 1	Control cell line 2
Figure 1B, C	X	
Figure 1D	X	X
Figure 1E	X	X
Figure 1F, G	X	
Figure 2	X	
Figure 3	X	
Figure 4 A	X	
Figure 4 B-F	X	X
Figure 5	X	X
Figure 6B, C	X	
Figure 6D-G	X	X
Figure 7	X	X

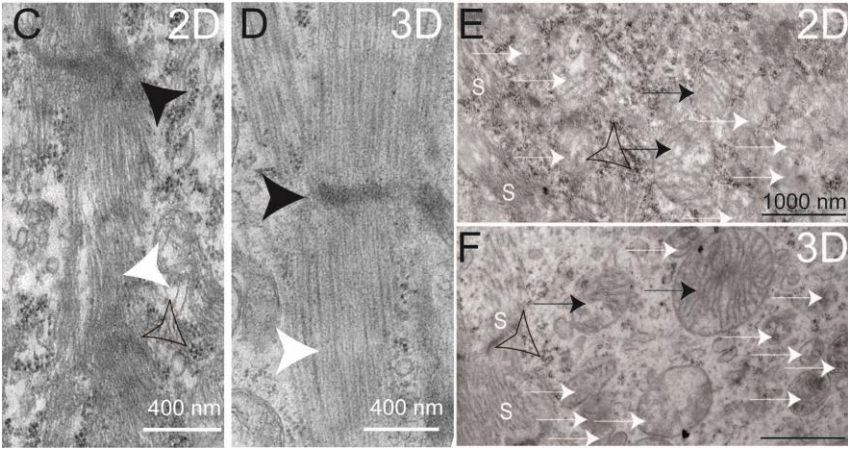
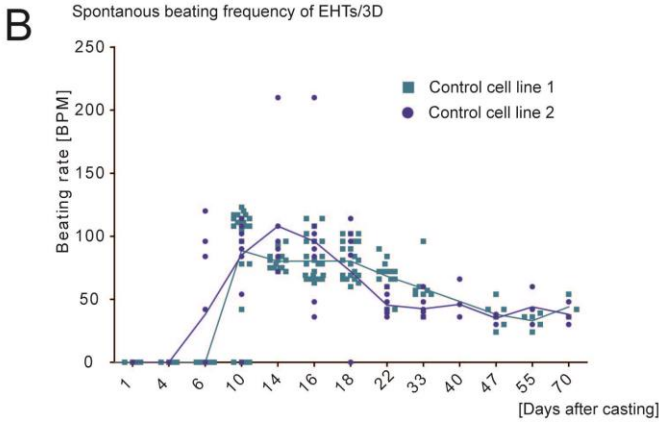


Figure S1: Overview of control cell lines (supplementary to Figure 1).

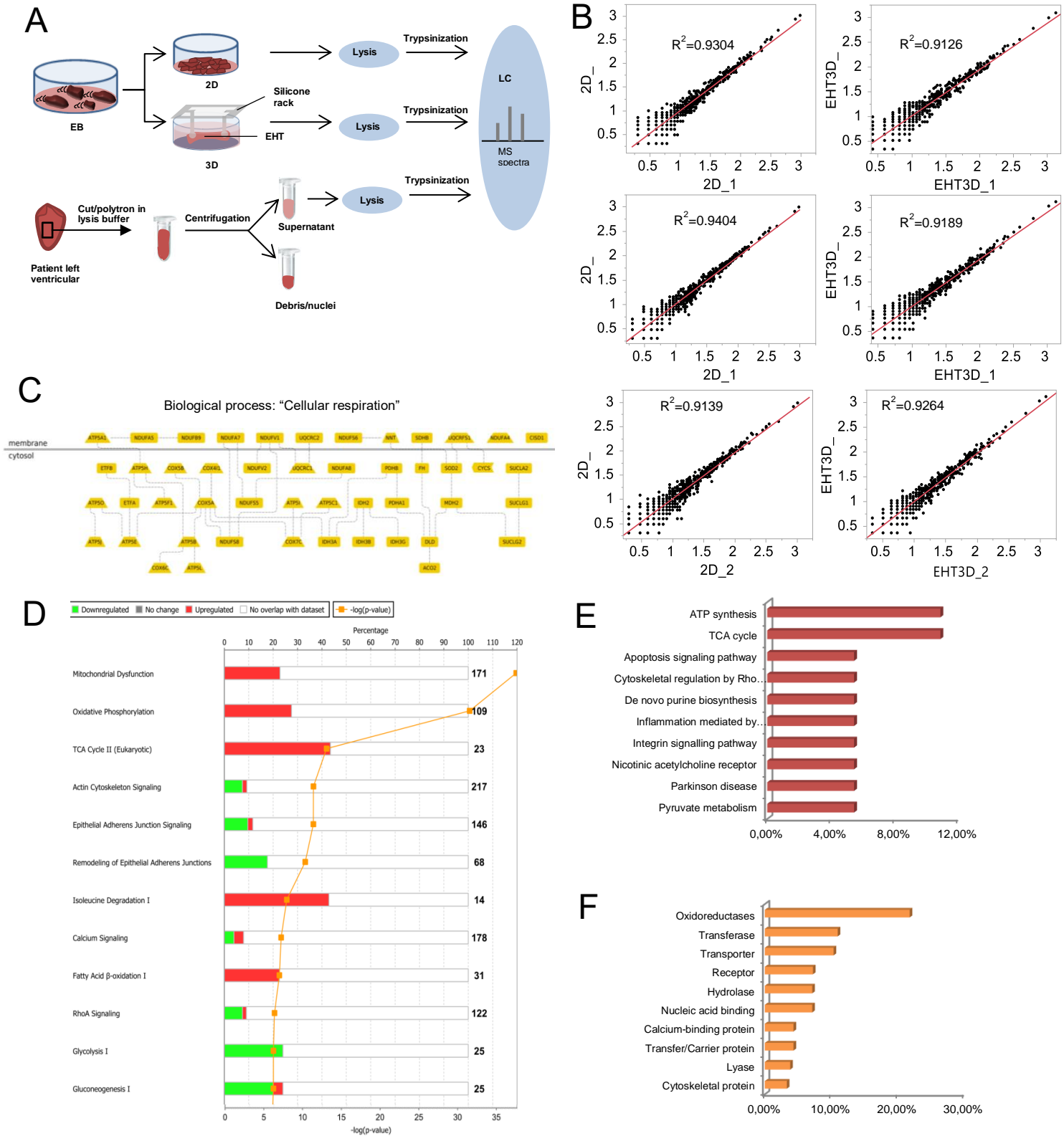
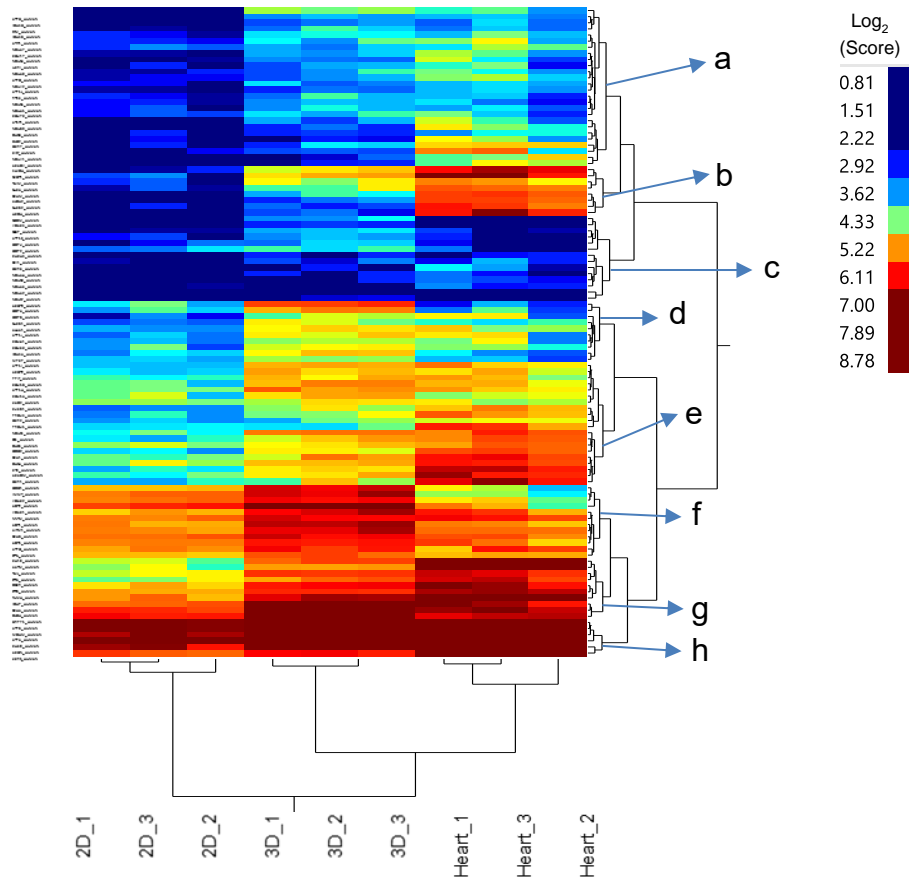


Figure S2: Work flow of mass spectrometry and protein ontology/canonical pathway analyses (supplementary to Figure 2).

A



B

Cluster	GO Biological Process	KEGG Pathway	Score
a	Mitochondrial electron transport, NADH to ubiquinone	Oxidative phosphorylation	12,86
	ATP biosynthetic process		4,32
	Tricarboxylic acid cycle	Citrate cycle	2,27
b	Metabolic pathways	Oxidative phosphorylation	4,46
	Fatty acid beta-oxidation	Fatty acid metabolism/Lysine degradation	3,78
	Response to activity	Valine, leucine and isoleucine degradation	3,63
c	Mitochondrial electron transport, NADH to ubiquinone	Oxidative phosphorylation	5,91
		Metabolic pathways	7,82
d	Tricarboxylic acid cycle	Citrate cycle (TCA cycle)	4,15
	Generation of precursor metabolites and energy	Oxidative phosphorylation	1,97
e	Mitochondrial electron transport, cytochrome c to oxygen	Oxidative phosphorylation/Cardiac muscle contraction	5,16
		Non-alcoholic fatty liver disease (NAFLD)	2,68
f	Transmembrane transport/Translation	Calcium signaling pathway	3,89
	Transmembrane transport	Calcium signaling pathway	3,39
		Metabolic pathways	2,56
g		Metabolic pathways	5,26

Figure S3: Gene ontology and KEGG pathway analysis performed for specific clusters (supplementary to Figure 3).

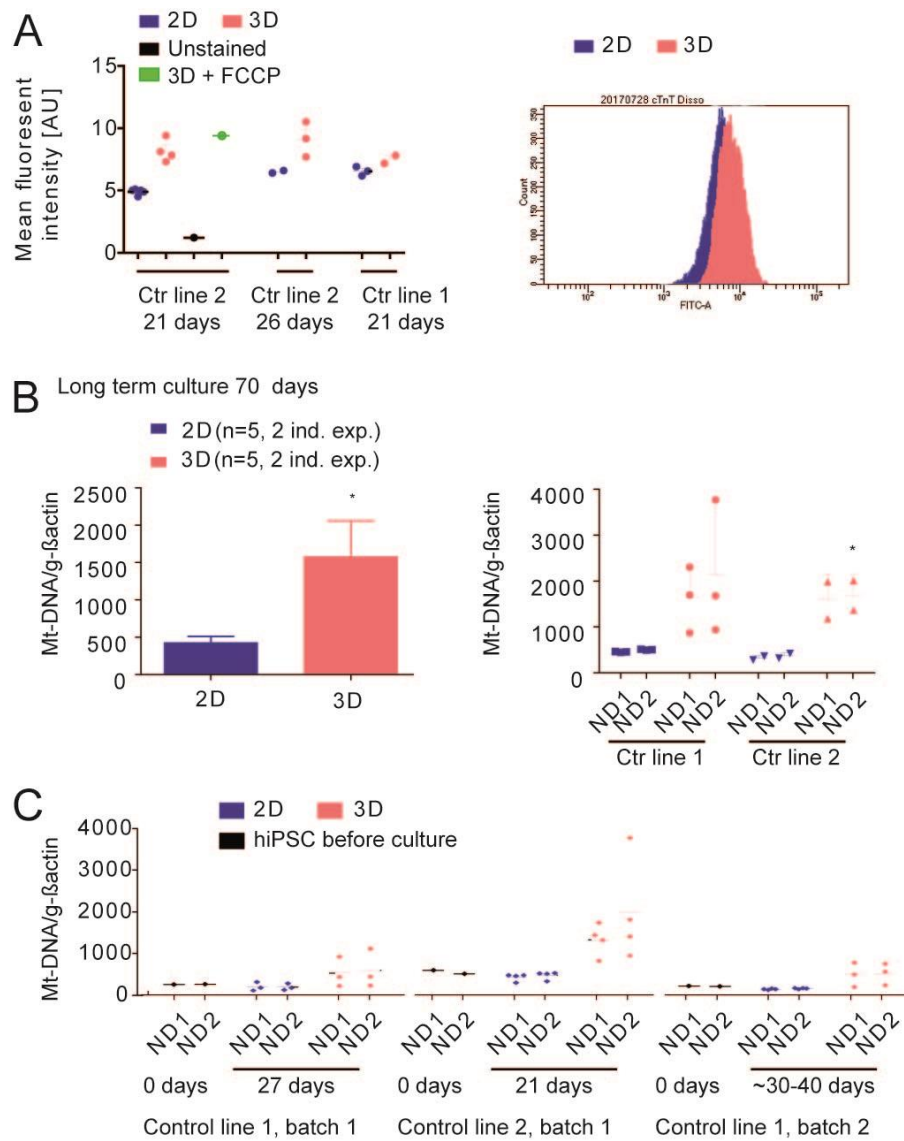


Figure S4: Analysis of mitochondrial DNA content and mass (supplementary to Figure 4).

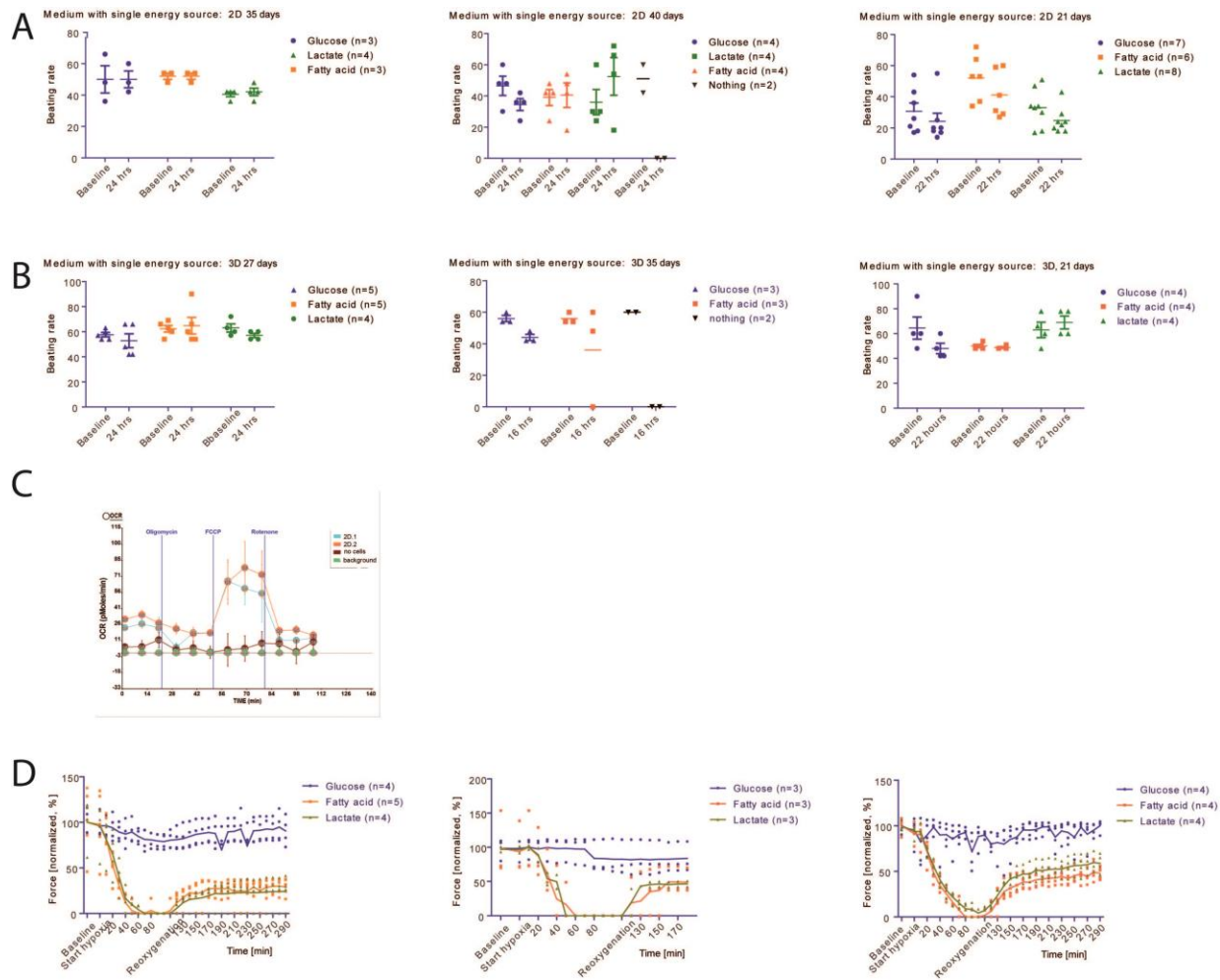


Figure S5: Depiction of different cell lines for contractile parameters such as force and beating rate and bioenergetic analysis utilizing the Seahorse XF24 analyzer and the extracellular flux assay kit (supplementary to Figure 5).

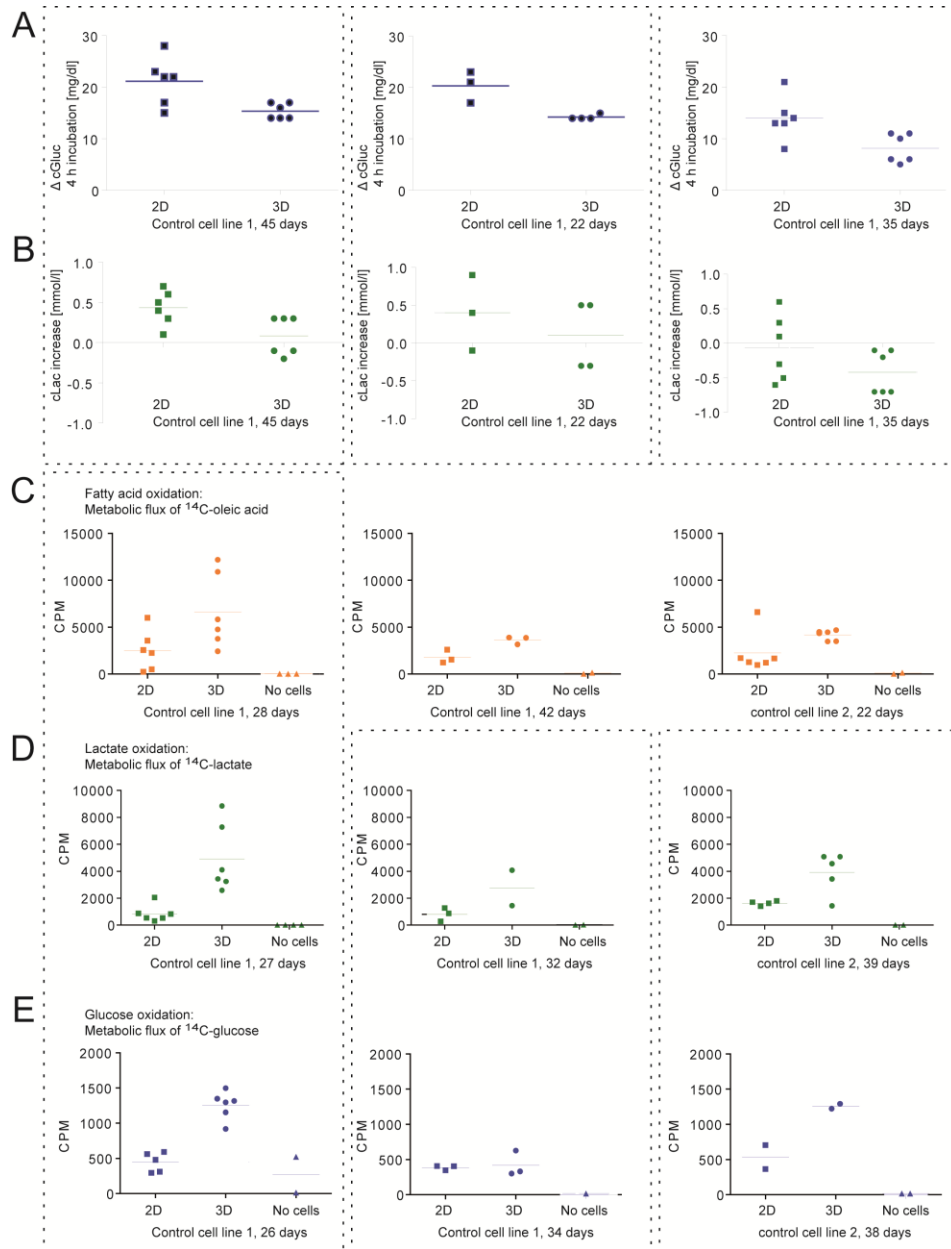
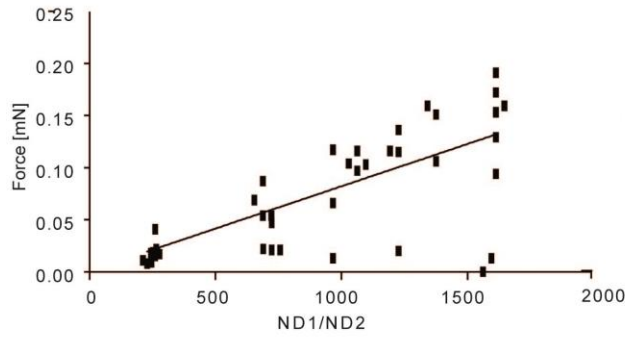
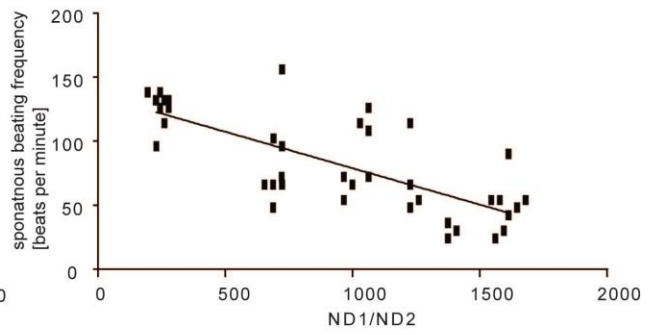


Figure S6: Depiction of raw data of independent experiments of both control cell lines for the analysis of metabolic flux (supplementary to Figure 6).

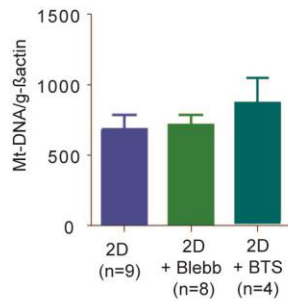
A 3D culture:
Correlation of mitochondrial DNA content and force



B 3D culture:
Correlation of mitochondrial DNA content and beating frequency



C 2D culture: Mitochondrial DNA content after blebbistatin/BTS treatment



D 2D culture: individual experiments, data combined in A.
Sample date: 21 days. Treatment between day 14-21.

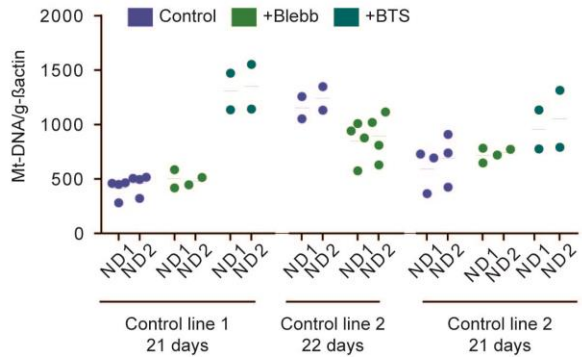


Figure S7: Analysis of mitochondrial DNA content (supplementary to Figure 7).

Legends for Supplemental Figures 1-7

Figure S1: Overview of control cell lines (supplementary to Figure 1).

(A) Overview of cell lines (control cell line 1: C25, (Moretti et al., 2010); ERC018, stem cell facility of the UKE, Hamburg) and experiments. (B) Baseline measurements in complete culture medium, spontaneous beating frequency (beats per minute) over time. Same EHTs shown in Figure 1C. Each dot represent one EHT. (C-F) Additional representative transmission electron microscopy pictures of 3D and 2D hiPSC-CM (open arrowhead in C, E, F: glycogen granules; black arrowhead: Z-line; white arrowhead: sarcomere; black arrow: mitochondria with features of maturity; white arrow: immature mitochondria).

Figure S2: Work flow of mass spectrometry and protein ontology/canonical pathway analyses (supplementary to Figure 2).

(A) Work flow of sample preparation for mass spectrometry. (B) Scatter plots of log₁₀ normalized spectral counts to characterize potential variance between samples per group. (C) Gene ontology (GO) analysis for biological processes determined by Genomatrix Genome Analyzer (GGA[®]) of proteins with significant higher abundance in 3D versus 2D. Demonstration of molecular targets (here named with the gene symbol) of top 1 hit “cellular respiration”. (D) Ingenuity Pathway Analysis (IPA[®]) of proteins significantly different between 2D and 3D. Demonstration of annotated pathways and sorting by the $-\log(p\text{-value})$. The p-value was calculated by IPA based on a Fisher’s exact test. The percentage characterizes the number of identified genes as being associated with each pathway. The number characterizes the total number of genes annotated with each pathway. Targets in green are considered to be downregulated in 3D, targets in red are considered to be upregulated in 3D. (E-F) Panther analysis for involved pathways of proteins with higher abundance in 3D (E) and involved protein classes (F).

Figure S3: Gene ontology and KEGG pathway analysis performed for specific clusters (supplementary to Figure 3).

(A) Cluster analysis of 2D, 3D and non-failing human heart were subjected to gene ontology and KEGG pathway enrichment analysis. Clusters are labeled from a-g. (B) Clusters from a-g with respective gene ontology (GO) and KEGG pathway information and enrichment score. Only significant enrichment scores > 1.5 were selected.

Figure S4: Analysis of mitochondrial DNA content and mass (supplementary to Figure 4).

(A) Mean fluorescent intensities of 2D vs. 3D for mitotracker green FM live stain depicted for different control (ctr) cell lines and 3 individual experiments. Each dot represents 1 experiment with pool of cells from 3 dissociated EHTs. FCCP treatment: Addition of 1 μM FCCP, 5 minutes pre-treatment before staining and during Mitotracker green FM live stain. Overlay of representative flow cytometry peaks (2D versus 3D). (B, C) PCR-amplification of genomic DNA for NADH dehydrogenase (Mt-ND1/2) normalized to the nuclear encoded gene actin; samples generated from 2 independent experiments. (B) mtDNA content (Mt-ND1, ND2) normalized to the nuclear encoded gene actin) after 70 days of culture time. Left panel: means \pm SEM, right panel: Scatter dot plot depiction of left panel, each dot represents one biological replicate and the mean of three technical replicates; statistical analysis: (B, left) two-tailed, unpaired t-test between 2D and 3D, (B, right) two-way ANOVA with Bonferroni post test. *: $p \leq 0.05$. (C) PCR-amplification of genomic DNA for NADH dehydrogenase (Mt-ND1/2) normalized to the nuclear encoded gene actin of 2D versus 3D hiPSC-CM. Scatter dot plot depiction of 3 independent experiments, mean of this data is presented in Figure 4F. Each dot represents one biological replicate, mean of 3 technical replicates.

Figure S5: Depiction of different cell lines for contractile parameters such as force and beating rate and bioenergetic analysis utilizing the Seahorse XF24 analyzer and the extracellular flux assay kit (supplementary to Figure 5).

(A, B) Cell line specific depiction of experiments shown in Figure 5A, B. (C) Measurements of respiration rates (ocr, oxygen consumption rate) per 20 000 2D plated cardiomyocytes per well in XF assay medium with sodium pyruvate (1 mM), L-glutamine (4 mM) and galactose (10 mM). Basal respiration, endogenous rate; oligomycin (1 μM); FCCP (0.5 μM); Rotenone (2 μM); samples generated from 1 experiments. (D) Cell line specific depiction of experiments shown in Figure 5C.

Figure S6: Depiction of raw data of independent experiments of both control cell lines for the analysis of metabolic flux (supplementary to Figure 6).

(A, B) Raw data (CPM of radioactive CO₂ trapped in filter paper) of individual experiments. Dashed boxes define independent experiments. Same data depicted as mean ± SEM displayed in Figure 6B, C. (C-E) Raw data (CPM of radioactive CO₂ trapped in filter paper) of independent experiments. Same data depicted as mean ± SEM displayed in Figure 6 D, E, F. Dashed boxes define experiments conducted with hiPSC-CMs derived from the same differentiation batch but at different time points. Each dot represents one biological replicate, mean of 2 technical replicates.

Figure S7: Analysis of mitochondrial DNA content (supplementary to Figure 7).

(A, B) Correlation of mitochondrial DNA content with force (A), and frequency (B) of experiments shown in Figure 7. (C, D) PCR-amplification of genomic DNA for NADH dehydrogenase (*Mt-ND1/2*) normalized to the nuclear encoded gene actin of 2D ± Blebbistatin (Blebb) and ± BTS. (C) Means ± SEM (D) Scatter dot plot depiction of left panel, each dot represents one biological replicate (mean of three technical replicates) from three independent experiments.

Supplemental Experimental Procedures

Human heart samples

Non-failing left ventricular myocardium utilized in Fig. 3 was obtained from 3 female donor hearts (National Disease Resource International; Philadelphia, PA) that could not be used for transplantation due to technical problems or the age of the donor. All non-failing hearts were normal in size and had no infarcts. Random sections had normal histology. Full details of the samples are previously described (Steenbergen et al., 2003). The heart samples in Fig. 4 were composed of one non-failing heart sample and two failing heart samples. Failing hearts were obtained from patients undergoing heart transplantation due to terminal heart failure caused by dilative cardiomyopathy or ischemic heart disease. Tissues from one non-failing donor heart that could not be transplanted was used for comparison. The study was reviewed and approved by the Ethical Committee of the University Medical Center Hamburg-Eppendorf (Az. 532/ 116/9.7.1991) and all patients gave written informed consent.

Sample preparation for mass spectrometric analysis

HiPSC-CM were cultured in either 2D (2×10^6 cells/6-well; coating: 0.1% gelatin, 1 h) or 3D (0.8×10^6 cells/EHT) for 21 days in parallel. Finally, cells were washed twice with PBS and digested with collagenase II (in HBSS, 200 U/ml; Worthington) for 4–5 h, reaction was stopped with fetal calf serum, centrifugated at 100 g for 15 min and washed twice with PBS. Cells of one 6-well or cells of 2 EHTs were snap frozen in 100 μ l M-PER Mammalian Protein Extraction Reagent plus phosphatase and protease inhibitors (Thermo Scientific). Frozen human heart samples were cut into pieces and lysed in an ice-cold buffer containing sucrose 300 mM, HEPES-NaOH 250 mM, EDTA 1 mM, pH 8, plus EDTA-free protease inhibitor (Roche). The tissue was homogenized using a tissue disruptor (Precellys 24, setting 6500-2x20-020) at 4°C and the samples were incubated for 15 min on ice. Insoluble cell debris was pelleted (14,000 rcf for 20 min) and the resulting supernatant was used for analysis. Protein concentrations in all sample groups were measured with a BCA protein assay kit (Pierce). 100 μ g of each sample lysate was used for acetone precipitation of proteins by adding the 8x volume of acetone (-20 °C, overnight). The next day, precipitated proteins were pelleted (high speed spin, 12 °C, 10 min). The acetone was removed and the dry protein pellet was dissolved in guanidine hydrochloride (8 M, solution ready to use, Sigma G9284). The protein pellet was subjected to an in-solution-digestion. Briefly, the mixture was reduced using dithiothreitol (10 mM, DDT, Sigma 43815) in 25 mM TEA-Bic solution (25 mM triethylammonium bicarbonate, Sigma T7408) for 1 h at 60°C. Samples were subjected to alkylation (30 mM iodoacetamide, Sigma I1149) in 25 mM TEA-Bic solution for 1 h at 37 °C in the dark. The reaction was quenched with DTT (10 mM, Sigma 43815). Afterwards, the samples were diluted with 25 mM TEA-Bic solution to a concentration of guanidine hydrochloride <1 M. The samples were digested overnight at 37°C in digestion buffer containing Sequencing Grade Modified Trypsin (1 μ g/ μ l, protein:enzyme ratio of approximately 20:1; Promega v5111). The next day, the tryptic peptides were acidified with 100% of formic acid to pH < 3. The samples were desalted and concentrated with ZipTip Pipette Tips (Millipore, ZTC18S096) filled with a C-18 column as described in the manufacturer's instructions. The collected eluents were vacuum-dried by SpeedVac and resolubilized in 0.1% formic acid.

Data analysis of mass spectrometry

MS2 spectra were processed using the Proteome Discoverer software (version 1.4.1.14, Thermo Fisher Scientific). Briefly, the data was searched against the Swiss Prot (Swiss Institute of Bioinformatics) database, taxonomy "Homo sapiens [human]" using the Mascot (Matrix Science, London, UK) search engine with precursor mass tolerance at 20 ppm, fragment ion mass tolerance at 0.8 Da, trypsin enzyme with 2 miscleavages with carbamidomethylation of cysteine as fixed modification and deamidation of glutamine and asparagine, oxidation of methionine as variable modifications. The resulting data file was loaded into the Scaffold software (version scaffold_4.3.4, Proteome Software Inc., Portland, OR, USA) to filter and quantify the peptides and proteins. For protein identification, filters were set to a 90% protein probability threshold and a 90% peptide probability threshold, which resulted in a final decoy FDR of less than 0.1%. For protein identification, at least 2 peptides per protein had to be recognized. Data analysis and clustering was performed in the Scaffold software. In general, relative quantification was done in a label-

free approach by the setting Quantitative Value (Normalized Total Spectra). For comparison, the total number of spectral counts identified for each proteins were visualized and compared to the counterpart. For statistical analysis only proteins identified in 3/3 samples were used for comparative analysis. For a quantitative analysis of specifically unique peptides to precisely distinguish between protein isoforms, the measured peak areas from Proteome Discoverer were analyzed using Scaffold and the Multiplex Quantitation method. Protein FDR was set to 1.0% and Peptide FDR to 0.1% with a minimum of 2 peptides. Quantitative analysis was performed by adjusting the reference group to the 2D samples. To display the comparison the setting was adjusted to fold change ratio. No minimal fold change threshold was applied.

Pathway, regulator effects and protein class analysis of differentially expressed proteins

Proteins identified as being significantly different between 2D- and 3D-cultured hiPSC-CM underwent canonical pathway analysis by the Ingenuity Pathway Analysis (IPA[®]) software. Evaluated were their annotation to canonical pathways and the sorting was performed by the $-\log(p\text{-value})$. The p-value was calculated by IPA[®] based on a Fisher right-tailed exact test. $P < 0.05$ was considered as statistically significant. Additionally, proteins which were significantly different between 2D and 3D underwent the analysis of regulator effects by IPA[®] and the effector networks with the highest consistency scores were determined. PANTHER pathway classification system (<http://www.pantherdb.org/pathway/>) was used for protein class analysis of proteins that were significantly enriched in 3D samples.

Sample preparation and Western blot

2D and 3D sample lysates, which were used for mass spectrometric analysis, underwent Western blot analysis. Equivalent amounts of protein (25 μg) from each sample were separated on NuPAGE 4–12% Bis-Tris gels (Invitrogen, Carlsbad, USA) and transferred to nitrocellulose membranes. Gel transfer efficiency and equal load was verified using reversible Ponceau staining. The resulting blots were probed with an anti-THIM (ACAA2, sc-100847, Santa Cruz, USA) antibody (1:200 dilution), an anti-ATP5H (ab110275, Abcam, USA) antibody (1:1000 dilution), an anti-COX-Va (MS409, Mito Sciences, USA) antibody (1:1000 dilution) to probe for mitochondrial proteins involved in β -oxidation and respiration. Membranes were probed with an anti- β -actin antibody to verify equal loading (sc-47778, Santa Cruz, USA). The membranes were incubated with a secondary antibody coupled with HRP conjugate targeted against mouse (7076S, Cell Signaling, USA) or rabbit (7074S, Cell Signaling, USA) and analyzed with ECL (GE Healthcare). Quantification of the bands was performed using ImageJ.

Flow cytometry

EBs, 2D and 3D samples were collagenase dissociated and 200 000 cells each were fixed in methanol and stained with anti-cardiac troponin T-FITC (Miltenyi, clone REA400) as previously described (Mannhardt et al., 2016). REA Control (I)-FITC was used for an isotypic control staining. Mitochondrial mass was detected by flow cytometry of collagenase dissociated living single cells, stained for 30 minutes in 0.5 μM MitoTracker Green FM (M7514, Molecular Probes). Unstained cells served as control. All flow cytometry was done in the UKE core facility with a BD FACSCanto[™] II (Biosciences) cytometer.

Quantitative PCR for relative mitochondrial DNA content and PGC1alpha/ESSRA

Experimental procedure and primer sequences as published in (Burkart et al., 2016). In brief, genomic and mitochondrial DNA was extracted from the organic phase after separation in Trizol by DNA precipitation with ethanol. DNA was washed twice with 0.1% sodium citrate/10% ethanol solution and with 75% ethanol. Pellet was dissolved in sterile water shaking over night at 37°C. Quantitative PCR was done on the AbiPrism 7900HT Fast Real-Time PCR System (Applied Biosystems) utilizing SYBR Green/ROX qPCR Master Mix (K0222, Thermo Scientific), using primers for mitochondrially encoded NADH dehydrogenase 1 (mt-ND1) or 2 (mt-ND2); values were normalized to the nuclear gene ACTB. Primer sequences as described in (Burkart et al., 2016): mt-ND1for: 5'-ATGGCCAACCTCCTACTCCTCATT-3' mt-ND1rev: 5'-TTATGGCGTCAGCGAAGGGTTGTA-3'; mt-ND2for:

5'-CCATCTTTGCAGGCACACTCATCA-3'; mt-ND2rev: 5'-ATTATGGATGCGGTTGCTTGCCTG-3'; ACTB (actin, beta) ACTB_for: 5'-CATGTACGTTGCTATCCAGGC-3', ACTB_rev: 5'-CTCCTTAATGTCACGCACGAT-3'. Values represent the mean of 3 technical replicates. RNA was extracted from the aqueous phase with a isopropanol precipitation. 500 ng of RNA were transcribed into cDNA with the High-Capacity cDNA Reverse Transcription Kit (4368814, Thermo Fisher). Controls without reverse transcription (-RT) served as negative controls. ESRR_for: 5'-GCCCTCACTACACTGTGTGAC-3'; ESRR_rev: 5'-CCTGCTAATTTGGACTGGTCTT-3'; PGC_for: 5'-CAGGCGATGGTGCAACTCATA. PGC_rev: 5'-CAGAGCACGTCCTTGAGCCA-3'. TNT for: CTGGAGAGAGGACGAAGACG, TNT rev: TTTGGTTTGGACTCCTCCAT; MYL3 for: AAGCCTTCATGCTGTTTCGAC, MYL3 rev: GCCTGTGTCCTTGTCTTGG; MYL4 for: CCACGTCTCTCGGTTTCTTCTT, MYL4 rev: CTCTTCAATCTGGTCGGCAGT, Vimentin for: GCAGGAGGAGATGCTTCAGA, Vimentin rev: GCAGCTCCTGGATTTCTCT; Periostin for: GAGGCTTGGGACAACCTTGA, Periostin rev: ACAGTGACAACCCATTAGGA; CD31 for: GGTCTGAGGGTGAAGGTGA; CD31 rev: GGGTTTGCCTCTTTTCTC. Glucuronidase beta GUSB_for: 5'-AAACGATTGCAGGGTTTCAC-3'; GUSB_rev: 5'-CTCTCGTCGGTGAAGGTGA-3'.

Transmission electron microscopy

For transmission electron microscopy (TEM), 3D and 2D-cultured hiPSC-CM were washed twice in PBS and fixed 30 min in glutaraldehyde (0.36%, pH 7.0-7.5, 4 °C). Prefixed 2D cells were removed as a full layer by scraping and pelleted. Prefixed EHTs were removed from silicone racks and further fixed in glutaraldehyde in osmium tetroxide solution (1%, 2 h; Science Services, 19110), dehydration and embedding in a glycidether-based resin. Ultra-thin sections (50 nm) were prepared and analyzed on a Zeiss LEO 912AB.

Restrictive feeding experiments

Baseline beating rate was analyzed in fresh complete medium. 2D and 3D-cultured hiPSC-CM were washed twice in DMEM without glucose (7455, Gibco) and then incubated for 10 min in 1.5 ml of the respective single-energy containing media. The medium was replaced once again and cells were incubated until the next day (22-26 hours of incubation). At the end of the experiment, beating frequency was analyzed again. For 3D, frequency and force was determined by video-optical recording before and after incubation. For 2D, frequency was determined by marking 2 foci (technical replicates) per 24-well containing 0.8x10⁶ hiPSC-CMs. Contractions per minute were counted microscopically for each foci before and after incubation. 3-4 wells (biological replicates) per condition were analyzed, 2D data represents mean of the two foci.

Hypoxia and reoxygenation treatment

3D cultured hiPSC-CM were pre-incubated in the respective single-energy containing medium as described in restrictive feeding experiments. Baseline was measured in the EHT analysis equipment (A001, EHT Technologies) by video-optical recording with a gas flow of CO₂ 35 ml/min, N₂ 265 ml/min, O₂ 200 ml/min. Gas composition was changed (CO₂ 35 ml/min, N₂ 465 ml/min, O₂ 0 ml/min) After 100 minutes oxygen supply was switched on again (CO₂ 35 ml/min, N₂ 265 ml/min, O₂ 200 ml/min), allowing reoxygenation.

Analysis of glucose consumption and lactate production

2D and 3D hiPSC-CM in 24 well format with 800 000 hiPSC-CM per sample were washed and then incubated for 10 min in 1.5 ml serum free full medium each. The medium was replaced once again and cells were cultured for 4 hours of incubation. Supernatant medium was collected and cGluc (concentration of glucose) as well as cLac (concentration of lactate) was measured utilizing a blood gas analyzer ABL90 blood gas analyzer (Radiometer). Glucose consumption was calculated as the initial cGluc of the medium before the 4 hours of incubation subtracted from cGluc after incubation. Lactate production was calculated by subtracting cLac after incubation from initial cLac.

Metabolic flux of ¹⁴C-labeled glucose, lactate and oleic acid

800 000 cells of either 2D or 3D hiPSC-CM per well were washed twice in serum-free full medium and then pre-incubated for 1 hour in serum-free full medium. After that, this medium was exchanged by serum-free full medium containing 0.0037 MBq/ml of one radioactive-labeled energy substrate and in addition 1 mM HEPES to ensure trapping of radioactive CO₂ in the buffered medium. While ¹⁴C-D-glucose (NEC042 PerkinElmer) and ¹⁴C-lactic acid (sodium salt, NEC599, PerkinElmer) was added directly to the incubation medium, ¹⁴C-oleic acid (NEC317, PerkinElmer) was brought into solution in a two-step procedure. First, at 54 °C all solvent was evaporated. Then, oleic acid was brought into solution by shaking it for one hour at 37 °C in full medium with 2% BSA as carrier. After 4 hours of incubation time allowing 2D and 3D hiPSC-CM to metabolize the isotope labeled energy substrates, 1 ml of supernatant was collected in a separate 24 well. 100 µl perchloric acid was added and immediately Whatman filter paper circles saturated with 3 M NaOH was placed on top of the wells. After 90 minutes of incubation in a closed chamber, Whatman filter paper was placed in 10 ml of Rotiscint eco plus (0016.3, Carl Roth) and the amount of radioactive CO₂ trapped in the filter paper was analyzed as counts per minute (CPM) in the liquid scintillation counter TriCarb 2900TR (Packard). Values represent means of two technical replicates. To calculate the amount of radioactive CO₂ produced, CPM was recalculated as decay per minute, Bq = CPM/60*96% (Figure 6 D-F) Total amount of radioactive CO₂ = bq /specific radioactivity per pmol (approximate values given by PerkinElmer: Glucose: bq x 1 pmol / 8 bq, oleic acid: Bq x 1 pmol / 2 bq, lactic acid: Bq x 1 pmol / 4 bq). The ATP production from fatty acid, lactate and glucose oxidation (Figure 6 G) was calculated based on metabolized energy substrate in relation to the input amount of substance:

Metabolized energy substrate = N/M*K; N = ¹⁴CO₂ [Bq]; M=Input radioactivity [¹⁴C-lactate, ¹⁴C-fatty acid, or ¹⁴C-glucose [Bq]]; K= Input amount of substance (Lactate, fatty acid or glucose [M]). The amount of ATP produced under assumption of a completely efficient production was calculated by multiplying the metabolized energy substrate with 33 per glucose molecule, and 15 per lactic acid molecule (Lopaschuk and Jaswal, 2010) 127,1 per oleic acid molecule (Peter C. Heinrich, Matthias Müller, 2014). As an alternative approximation to calculate glycolysis/oxidation ratios we used data from lactate production (Figure 6C) to calculate ATP production by anaerobic glycolysis. The increase in lactate (280 nM for 2D, 113 nM for 3D) is the sum of large lactate production and small lactate oxidation (1-3 nM, about 1% in our experiments, Figure 6C, G), which we ignored in the following calculations. Given that during anaerobic glycolysis 1 Glucose is broken down to 2 molecules of lactate producing 2 molecules of ATP, we can estimate the total production of ATP by anaerobic glycolysis with 280 nM for 2D and 113 nM for 3D.

Media composition and drug treatments

Complete medium was used to culture 2D and 3D hiPSC-CM. Medium was changed 3x per week and consisted of Dulbecco's MEM (F0415, Biochrom), 10% horse serum, inactivated (Biochrom), 1% penicillin/streptomycin (15140, Gibco), insulin (10 µg/ml, 857652, Sigma-Aldrich) and aprotinin (33 µg/ml, A1153, Sigma-Aldrich). Serum-free medium consisted of DMEM without D-glucose, without L-glutamine, and without sodium pyruvate (7455, Gibco), 1% penicillin/streptomycin (15140, Gibco), insulin (10 µg/ml, 857652, Sigma-Aldrich), 0.25 mM L-carnitine hydrochloride (C0283, Sigma) with the addition of 1 mM linoleic acid/oleic acid fatty acid mix (L9655, Sigma), 1 mM lactate (7455, Sodium lactate solution 50%, Caelo), 5 mM D (+)-glucose anhydrous (X997, Roth). Single energy substrate media for restrictive feeding experiments were prepared as specified above, but only one of the energy sources was added. (S)-(-)- Blebbistatin (SC-204253, Santa Cruz, stock concentration: 10 mM in DMSO, was freshly diluted to 300 nM in complete medium) or N-benzyl-p-toluene sulphonamide (BTS, 1870, Tocris, stock 30 mM in DMSO, was freshly diluted to 20 µM in complete medium with daily medium change during the 7 day incubation period between day 14 and day 21 of hiPSC-EHT development. Concentration on BTS and Blebbistatin were chosen on a approximative 50% reduction of contractile force in 3D. These concentrations align well with literature data (Cheung et al., 2002; Straight et al., 2003). The same concentrations also led to a substantial weaker contraction in 2D, as observed in light microscopy.

Supplemental References

Burkart, A.M., Tan, K., Warren, L., Iovino, S., Hughes, K.J., Kahn, C.R., and Patti, M.-E. (2016). Insulin Resistance in Human iPS Cells Reduces Mitochondrial Size and Function. *Sci. Rep.* 6, 22788.

Cheung, A., Dantzig, J.A., Hollingworth, S., Baylor, S.M., Goldman, Y.E., Mitchison, T.J., and Straight, A.F. (2002). A small-molecule inhibitor of skeletal muscle myosin II. *Nat. Cell Biol.* 4, 83–88.

Lopaschuk, G.D., and Jaswal, J.S. (2010). Energy Metabolic Phenotype of the Cardiomyocyte During Development, Differentiation, and Postnatal Maturation. *J. Cardiovasc. Pharmacol.* 56, 130–140.

Mannhardt, I., Breckwoldt, K., Letuffe-Brenière, D., Schaaf, S., Schulz, H., Neuber, C., Benzin, A., Werner, T., Eder, A., Schulze, T., et al. (2016). Human Engineered Heart Tissue: Analysis of Contractile Force. *Stem Cell Reports* 7, 29–42.

Moretti, A., Bellin, M., Welling, A., Jung, C.B., Lam, J.T., Bott-Flügel, L., Dorn, T., Goedel, A., Höhnke, C., Hofmann, F., et al. (2010). Patient-Specific Induced Pluripotent Stem-Cell Models for Long-QT Syndrome. *N. Engl. J. Med.* 363, 1397–1409.

Peter C. Heinrich, Matthias Müller, L.G. (2014). *Löffler/Petrides Biochemie und Pathobiochemie* (Berlin, Heidelberg: Springer Berlin Heidelberg).

Steenbergen, C., Afshari, C.A., Petranka, J.G., Collins, J., Martin, K., Bennett, L., Haugen, A., Bushel, P., and Murphy, E. (2003). Alterations in apoptotic signaling in human idiopathic cardiomyopathic hearts in failure. *Am. J. Physiol. - Hear. Circ. Physiol.* 284.

Straight, A.F., Cheung, A., Limouze, J., Chen, I., Westwood, N.J., Sellers, J.R., and Mitchison, T.J. (2003). Dissecting temporal and spatial control of cytokinesis with a myosin II Inhibitor. *Science* 299, 1743–1747.

Supplemental Information for legends of the video files

Movie S1

Video documentation of hiPSC-CM in EB format at the end of differentiation, 2D monolayer and 3D EHT format. Supplemental to Figure 1.

Movie S2

Video documentation of hiPSC-CM in EHT format in restrictive feeding experiment (Supplemental to Figure 5): EHTs supplemented with glucose, lactate or fatty acid cultivated in normoxia and hypoxia.